LUNAR ORBIT RENDEZVOUS REFERENCE TRAJECTORY DATA PACKAGE (U)

PREPARED UNDER CONTRACT NO. 10001
TO BELLCOMM, INC.

ANALYSIS OF APOLLO ORBIT DETERMINATION ACCURACY WITH RANDOM ERRORS IN GROUND BASED RADAR AND ONBOARD OPTICAL OBSERVATIONS

VOLUME 6

SUMMARY AND CONCLUSIONS

8408-6045-RC-000 **JULY 10, 1964**

TRW SPACE TECHNOLOGY LABORATORIES
THOMPSON RAMO WOOLDRIDGE INC.

SPACE TECHNOLOGY LABORATORIES, INC.
A SUBSIDIARY OF THOMPSON RAMO WOOLDRIDGE INC.
SPACE TECHNOLOGY CENTER · ONE SPACE PARK · REDONDO BEACH, CALIFORNIA

9880.2-13

August 10, 1964

Mr. R. L. Wagner, Head
Trajectory Department
Bellcomm, Inc.
1100 17th Street, N.W.
Washington 6, D. C.

Dear Mr. Wagner,

Following our telecon this morning concerning typographical errors in TRW Space Technology Laboratories Report No. 8408-6045-RC-000, "Analysis of Apollo Orbit Determination Accuracy with Random Errors in Ground Based Radar and Onboard Optical Observations, Volume 6, Summary and Conclusions", dated July 10, 1964, I had the document reviewed for any additional errors. The following is a "complete" list of errata:

1. Page 4, paragraph 2, line 4. The word "degraded" is mistakenly repeated.

2. Page 4, first paragraph, last sentence. Replace the last sentence with "The apparent anomaly of the degradation in accuracy being greater in the case of four or five radar passes as compared to the cases of sparse visibility is explained in Reference 2".

3. Page 6, paragraph 3, line 7. The number "30°" should read "130°".

4. Page 7, paragraph 3, last line. The number "6.2-1" should read "6.2.2-1".

5. Page 8. The figure title should read "Effects of Launch Azimuth, Type of Coast, and Time of Flight on Orbit Determination Using Optical Data".

6. Page 10. The figure title should read "Effects of Launch Azimuth, Type of Coast, and Time of Flight on Orbit Determination with Group II (with range data)".

7. Page 17. Add figure number and title: "Figure 6.2.3-1 Visibility of Moon from DSIF Stations (min. elev. angle = 5°)".

8. Page 25. Everywhere it appears (3 places) replace the symbol ψ with φ.

9. Page 36, first paragraph, line 2. The word "four" should read "three".

10. Page 38, Figure 6.3.1-1. The line R_1 should be a straight line from Station 1 to Vehicle. The Y axis should be perpendicular to X which in turn should bisect the angle included by R_1 and R_2.

11. Page 41, paragraph 3, line 5. The figure number 6.3.2-1 should read 6.3.1-3.

12. Page 41. Figure 6.3.2-1 should be Figure 6.3.1-3.

13. Page 42, line 2. The figure number 6.3.2-2 should read 6.3.1-4.

14. Page 42. Figure 6.3.2-2 should be Figure 6.3.1-4.

15. Page 42, first paragraph, line 5. The figure number 6.3.2-3 should read 6.3.1-5.

16. Page 42, first paragraph, line 6. The figure number 6.3.2-2 should read 6.3.1-4.

17. Page 42. Figure 6.3.2-3 should be Figure 6.3.1-5.

18. Page 44, middle of page. The first equation should be

$$\frac{1}{r\sqrt{\sigma_I^2 + \left(\frac{\sigma_L}{r}\right)^2}}$$

Although this document was proof read by the contributors and myself, there is an inordinate number of errors for which I apologize.

Sincerely yours,

TRW Space Technology Laboratories

Frederick L. Baker

Frederick L. Baker
Project Manager

FLB:jcb

~~CONFIDENTIAL~~ Copy ~~COPIES~~ of

Unclassified

LUNAR ORBIT RENDEZVOUS REFERENCE TRAJECTORY DATA PACKAGE (U)

Prepared Under Contract No. 10001
to Bellcomm, Inc.

ANALYSIS OF APOLLO ORBIT DETERMINATION ACCURACY WITH RANDOM ERRORS IN GROUND BASED RADAR AND ONBOARD OPTICAL OBSERVATIONS

VOLUME 6
SUMMARY AND CONCLUSIONS

8408-6045-RC-000 July 10, 1964

Classification changed to UNCLASSIFIED by authority of SCG-11, Rev. 1, 1/1/66, and SCG-6, 8/2/64, as amended
By [illegible] Date: 3-22-69
letter dated 3-11-69 from R. L. Wagner

Approved: F. L. Baker
F. L. Baker
Project Manager

Approved: for E. M. Boughton
E. M. Boughton
Assistant Director
for Projects
Mission Analysis and
Simulation Laboratory

~~DOWNGRADED AT 12 YEAR INTERVALS;~~
~~DECLASSIFIED AFTER 12 YEARS~~
~~DOD DIR 5200.10~~

Total Pages: 48

TRW SPACE TECHNOLOGY LABORATORIES
THOMPSON RAMO WOOLDRIDGE INC.
ONE SPACE PARK • REDONDO BEACH, CALIFORNIA

Unclassified

~~CONFIDENTIAL~~

ACKNOWLEDGEMENTS

The following personnel contributed to the preparation of this volume:

D. Dethlefsen
M. Pancino
R. Ellis
T. Sands
W. Pace

CONTENTS

6.1 INTRODUCTION

This volume is the last of a series describing the tracking accuracy, or orbit determination study performed by TRW Space Technology Laboratories, Inc., for Bellcomm, Inc., under Contract Number 10001 (Amendment 2).

Orbit determination consists of the reconstruction, or statistical estimation, of a trajectory from noisy observational data. Two general types of data were considered in this study: (1) radar data as obtained by ground based radar trackers and (2) optical observations taken onboard the spacecraft itself. The study consisted of a statistical error analysis, performed by means of digital computer simulations, of the accuracy to which the various free-flight portions of the overall trajectory could be determined using ground-based and onboard tracking systems separately and combined. The analysis was predicated on assumed error or noise models for the various types of measuring equipment—radars, telescopes, and sextants. These assumed errors were converted into equivalent errors in orbital parameters and these errors, in turn, were propagated along the trajectory to describe the uncertainty in position and velocity existing at various points on the trajectories.

The orbit determination scheme simulated was weighted least squares. This method is quite general and is related to—and in some cases equivalent to—other estimation techniques such as minimum variance, maximum likelihood and linear filtering, and is discussed in Reference 1.

However, it should be noted that the statistical analysis in this study was based on the assumptions that the observation errors were uncorrelated and unbiased with known variances, and that the physical model used is completely accurate. That is, only the orbit parameters are assumed to have uncertainties and all other parameters (except ship locations) are assumed to be known perfectly. The effects of data correlations and biases, uncertainties in physical constants, and drag or venting uncertainties are not included.

Trajectories were considered parametrically, to discover any dependence of orbit determination accuracy on various trajectory parameters such as inclination, altitude, flight time, location of nodes, etc. For example, in the earth

orbit phase, the dependence on launch azimuth, altitude, and number of revolutions was studied. Such trajectory parameters are important because they can influence (1) visibility to various ground-based tracking stations and (2) the manner in which errors propagate along the trajectories. An attempt was made to cover as nearly as possible, the complete range of these parameters which might be encountered in the Apollo mission.

The Apollo mission and tracking systems considered are described in Reference 1. References 2 through 5 give detailed discussions and results for each phase of the mission. The purpose of this volume is to summarize the results and to comment on some of the more important findings.

6.2 SUMMARY OF SIMULATION RESULTS

The principal results of the orbit determination study are given in the four subsections below, covering each of the mission phases studied and reported separately in References 2 through 5. Although complete descriptions of the simulations and results may be found in the appropriate references, all pertinent background information connected with the scope of the study is discussed below. Reference 1, containing all input data and applicable statistical theory, is intended to be used as a companion volume to this summary report.

6.2.1 The Earth Parking Orbit

An analysis of tracking accuracy for a vehicle in an earth parking orbit was accomplished by means of computer simulations of tracking data resulting from assumed tracking systems operating in conjunction with a given set of earth parking orbit configurations. The orbits were assumed to be circular at a nominal altitude of 100 nautical miles, and to correspond to launches from Cape Kennedy over a range of azimuths extending from 60 to 120 degrees. For each launch azimuth, epoch was defined as the instant of injection into the parking orbit, and was taken to mark the beginning of the first orbital revolution. Injection conditions were obtained from Reference 6. In order to explore the possible improvement in orbit determination accuracy resulting from the increase in visibility time associated with higher orbital altitudes, the effects of increasing altitude to 150 and 200 nautical miles were also investigated.

The basic method used in this determination of accuracy was to simulate the acquisition of tracking data over a specified tracking interval and then to propagate the generated covariance matrix of tracking accuracy to various future times. The tracking intervals used were the first orbital revolution, the second orbital revolution, and the combination of the first and second revolutions. The future times were chosen as the one-eighth-revolution time points in the orbital revolution immediately following the tracking period.

This procedure was carried out for two types of observations: Group I radar observations and optical observations. Group I radar tracking employed eight land-based radars and three shipboard radars (see Reference 1). This group was further divided into two cases: the "exact" case, in which ship locations were assumed to be known exactly; and the "uncertain" case, in which these locations were assumed to be known only to within specified uncertainties. In the latter case, the locations of the tracking ships were determined along with the orbit parameters. Onboard optical tracking data were obtained by measurements of the direction cosines of the landmark direction relative to the fixed orthogonal coordinate system associated with the onboard inertial platform.

The quantities chosen to indicate the accuracy with which position and velocity can be predicted were the root-semitraces in position and velocity. These are the square roots of the sums of the variances in position coordinates and in velocity components, respectively. For each trajectory and tracking interval, the root-semitraces in position and velocity were plotted as functions of time. Additionally, broad levels of tracking accuracy have been associated with the criteria of total visibility time and number of radar passes. A "radar pass" is defined as a single visibility period associated with one radar, i.e., one radar "look".

For the general case of tracking with the assumed earth-based radar network over either the first or second orbital revolutions, assuming ship locations to be known exactly, it was found that 1σ uncertainties in orbit prediction of within 100 feet in position and 0.1 feet per second in velocity may be obtained with four or five radar passes, corresponding to a total visibility time of approximately 13 - 19 minutes and to a launch azimuth in the range of 80 - 100 degrees.

When the tracking interval was extended over two orbital revolutions producing abundant visibility in the range of 11 to 16 radar passes, these accuracy figures were improved by a factor of four. When visibility was sparse, and only two or three radar passes were obtained, these figures were degraded by a factor of ten.

When ship locations were assumed to be known only to within the assumed uncertainties, the cases of abundant visibility produced accuracies equivalent to those of the exact cases, the case of four or five radar passes produced accuracies degraded by a factor of five compared to the exact cases of equivalent visibility, and the cases of sparse visibility were worse by a factor of two compared to the exact cases. The apparent anomaly of the degradation in accuracy being greater in the case of four or five radar passes as compared to the cases of sparse visibility is explained in Reference 2.

The increased visibility time resulting from a doubling of orbital altitude produced significant improvement in the accuracy of orbit determination. For the assumed uncertainty in the determination of landmark direction, tracking by means of onboard optical measurements alone was found to be characterized by levels of accuracy many times worse than those associated with earth-based radar tracking alone. For this reason a merger of the two types of tracking data would lead to negligible improvement in overall tracking accuracy. Table 6.2.1-I illustrates these conclusions with the numerical results of the study.

6.2.2 Translunar Trajectory

The analysis of orbit determination accuracy for the translunar free-flight phase of the Apollo mission consists basically of two parts: trajectory selection effects and tracking system effects. The theory applicable to this analysis is contained in Reference 1.

The parameters chosen for the analysis of trajectory selection effects are launch azimuth, type of earth orbital coast, flight time, launch date, and selenographic inclination of the lunar approach hyperbola. The type of earth orbital coast is defined as an integer specifying the opportunity for injection into the translunar trajectory out of the earth parking orbit and is used to indicate the length of the parking orbit coast. The translunar trajectory is required to be of

Table 6.2.1-I. Earth Parking Orbit – Overall Tracking Accuracy

	Ship Locations	Total Visibility Time (min)	Number of Radar Passes	RST Upper Bounds RST(R) (ft)	RST Upper Bounds RST(V) (ft/sec)
Earth-Based Radar Tracking Only (Data rate = 10 points per minute)	Uncertain	6-12	2-3	2,000	2.0
		13-19	4-5	500	0.50
		20-27	6-7	100	0.10
		28-37	8-10	50	0.050
		38-60	11-16	25	0.025
	Exact	6-12	2-3	1,000	1.0
		13-19	4-5	100	0.10
		20-27	6-7	70	0.07
		28-37	8-10	50	0.050
		38-60	11-16	25	0.025
	Tracking Interval, Orbital Revolution	Total Visibility Time (min)	Landmark Error (NM)		
Onboard Optical Tracking Only (Data rate = 0.1 point per minute)	1	88	1.0	20,000	22.0
	1 and 2	176	1.0	7,000	8.0
	1	88	0.1	2,000	2.2
	1 and 2	176	0.1	700	0.8

Note: All conclusions are based upon tracking data acquired over one and two orbital revolutions.

the free-return type; that is to say, it circumnavigates the moon and returns to earth with acceptable reentry conditions. The trajectories considered herein are not, in general, of the free-return type; however, this type is simply a set of trajectories having special combinations of the above parameters and, therefore, is covered by the results presented in this study.

The tracking systems considered herein are C-band ground-based radars, the Deep Space Instrumentation Facility (DSIF) S-band radars, and the onboard sextant. The characteristics of these systems are described in detail in Reference 1. The following configurations of these systems are considered:

(a) Group I (C-band); range, azimuth, elevation
(b) Group II (DSIF); range, azimuth, elevation, range rate
(c) Group II (DSIF); azimuth, elevation, range rate
(d) Group III (DSIF); range, azimuth, elevation, range rate
(e) Onboard optical measurements
(f) A combination of (c) and (e)

It should be emphasized that the optical model used gives lower uncertainties than the sextant will be able to achieve by measuring one angle at each observation time with the accuracies as stated in Reference 1. However, the uncertainty achievable by optimum one-angle measurements should be no more than 1.4 times that presented here.

The procedure used to study trajectory selection effects is to assign values to four of the trajectory parameters listed previously and to calculate state vector uncertainties as a function of time from translunar injection for a set of trajectories having several different values for the remaining parameter. The base point values assigned to the parameters are 90° launch azimuth, type 5 earth orbital coast, 70 hours flight time, January 22, 1968 launch date, and 130° selenographic inclination of the lunar approach hyperbola. The types of earth orbital coast used in this study have the following relations to orbital coast length: type 4, 1.0 to 1.5 revolutions; type 5, 1.5 to 2.0 revolutions; and type 6, 2.0 to 2.5 revolutions. For the study of the various tracking systems, the trajectory used was of the free-return type having 90° launch azimuth, type 5 earth orbital coast, 70 hours flight time, January 29, 1968 launch date, and 166° selenographic inclination of the lunar approach hyperbola.

The spacecraft state vector uncertainties presented have been propagated to lunar arrival or to reentry of a free-return trajectory. Those uncertainties propagated to lunar arrival are presented in the form of RST(R) and RST(V) which are the RSS of the standard deviations in the three position and velocity coordinates respectively, of an inertial Cartesian coordinate system. The quantitites RST(R) and RST(V) have the property of being invariant under rotations of the coordinate system axes. For data propagated to reentry, 1σ uncertainties are presented for flight path angle, arrival time, and velocity magnitude.

During the Apollo translunar phase, three midcourse corrections will be made based on the information obtained from tracking data in order to reduce terminal errors arising from an imperfect translunar injection. These corrections affect orbit determination through uncertainties in the trajectory introduced by imperfect measurement of the maneuver by instrumentation onboard the spacecraft. Since the maneuver is essentially impulsive, the uncertainties in position measured at the point of the correction will be unaffected by the maneuver. The position uncertainties measured at pericynthion, however, will be affected by the maneuver since velocity uncertainties propagate forward as both position and velocity uncertainties. A pessimistic estimate of the capability of the measurements is 0.1 meter per second in each inertial coordinate. These 1σ uncertainties are introduced at 10 hours from injection, at the entrance into the moon's sphere of influence, and at one hour prior to closest approach to the moon.

For Group II tracking (with range data), the significant effects of trajectory selection on tracking uncertainties are observed over the first few hours of the flight and are primarily a result of tracking coverage. The trajectory parameters affecting tracking accuracy at the first correction location are launch azimuth, type of earth orbital coast, flight time, and launch data. The tracking uncertainties over the latter portion of the trajectory are insensitive to trajectory variations. The optical tracking uncertainties are influenced by trajectory selection through the geometry of the trajectory with respect to the earth-moon system. Launch date, flight time, and selenographic inclination have effects on tracking uncertainties at the first midcourse correction location. The tracking uncertainties at the last two correction locations are sensitive to flight time as this parameter determines the amount of data available with a given sampling rate. Figures 6.2-1 through -4 present these sensitivities.

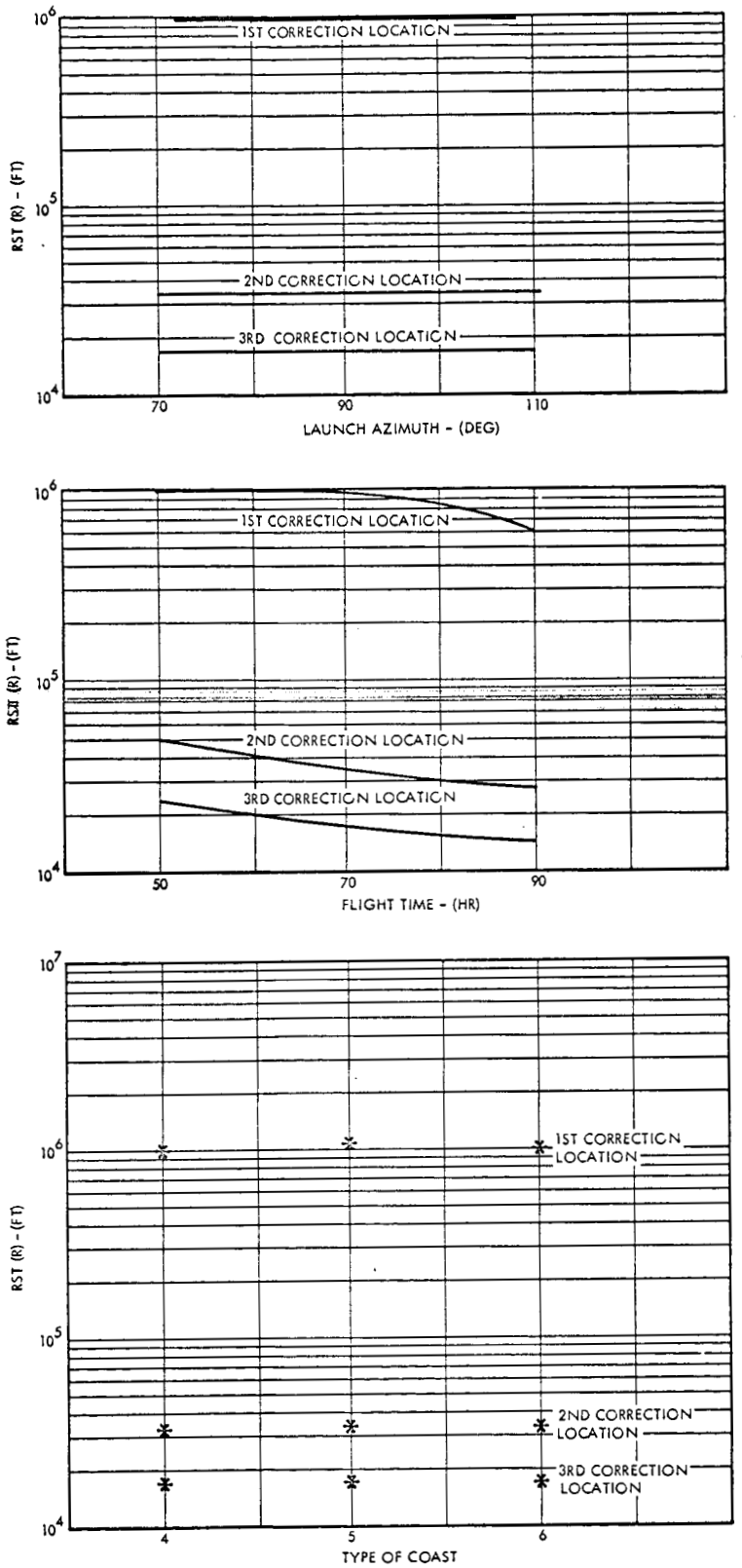

Figure 6.2.2-3. Effects of Launch Azimuth, Type of Coast, and Time of Flight on Orbit Determination Using Optical Data

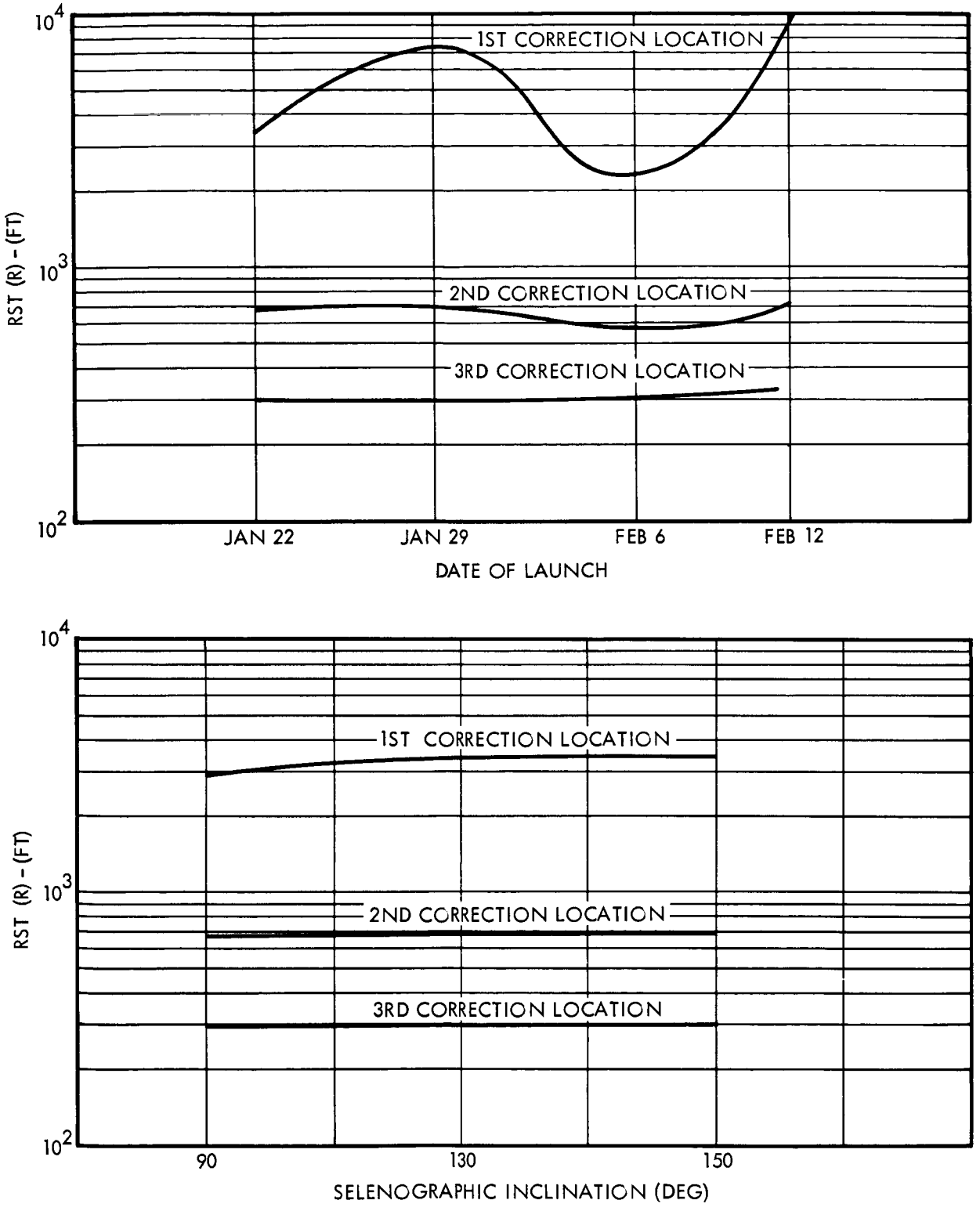

Figure 6.2.2-2. Effects of Date of Launch and Selenographic Inclination on Orbit Determination with Group II (with range data)

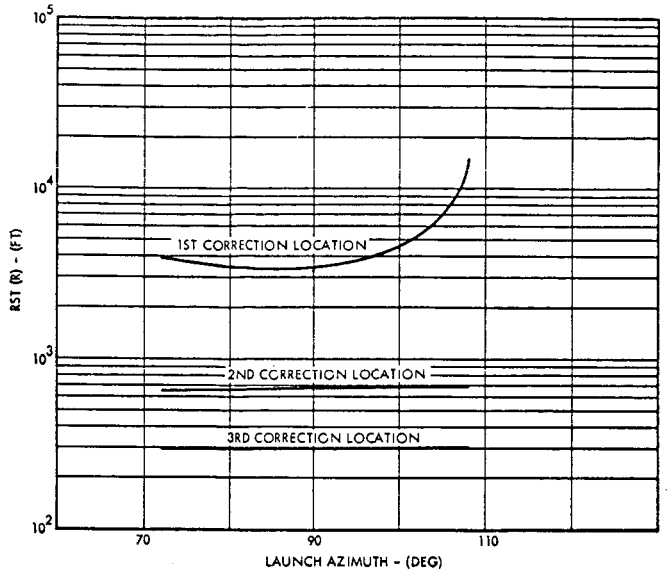

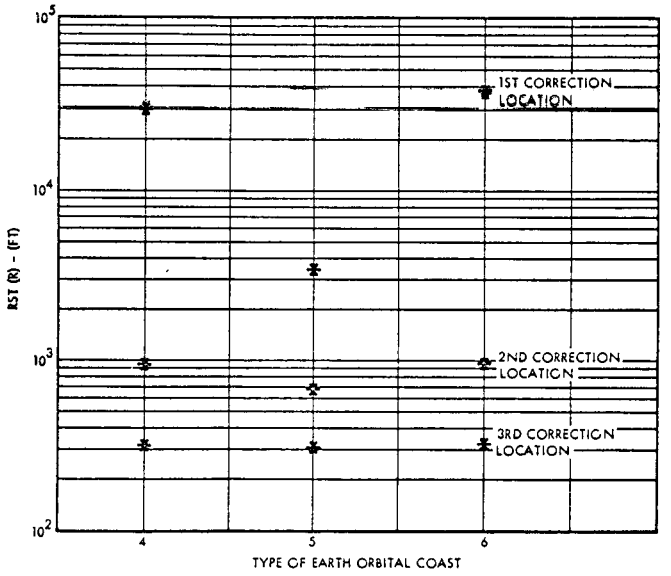

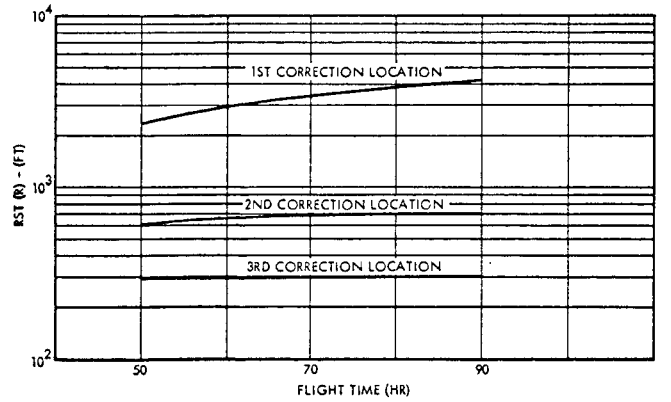

Figure 6.2.2-1. Effects of Launch Azimuth, Type of Coast, and Time of Flight on Orbit Determination with Group II (with range data)

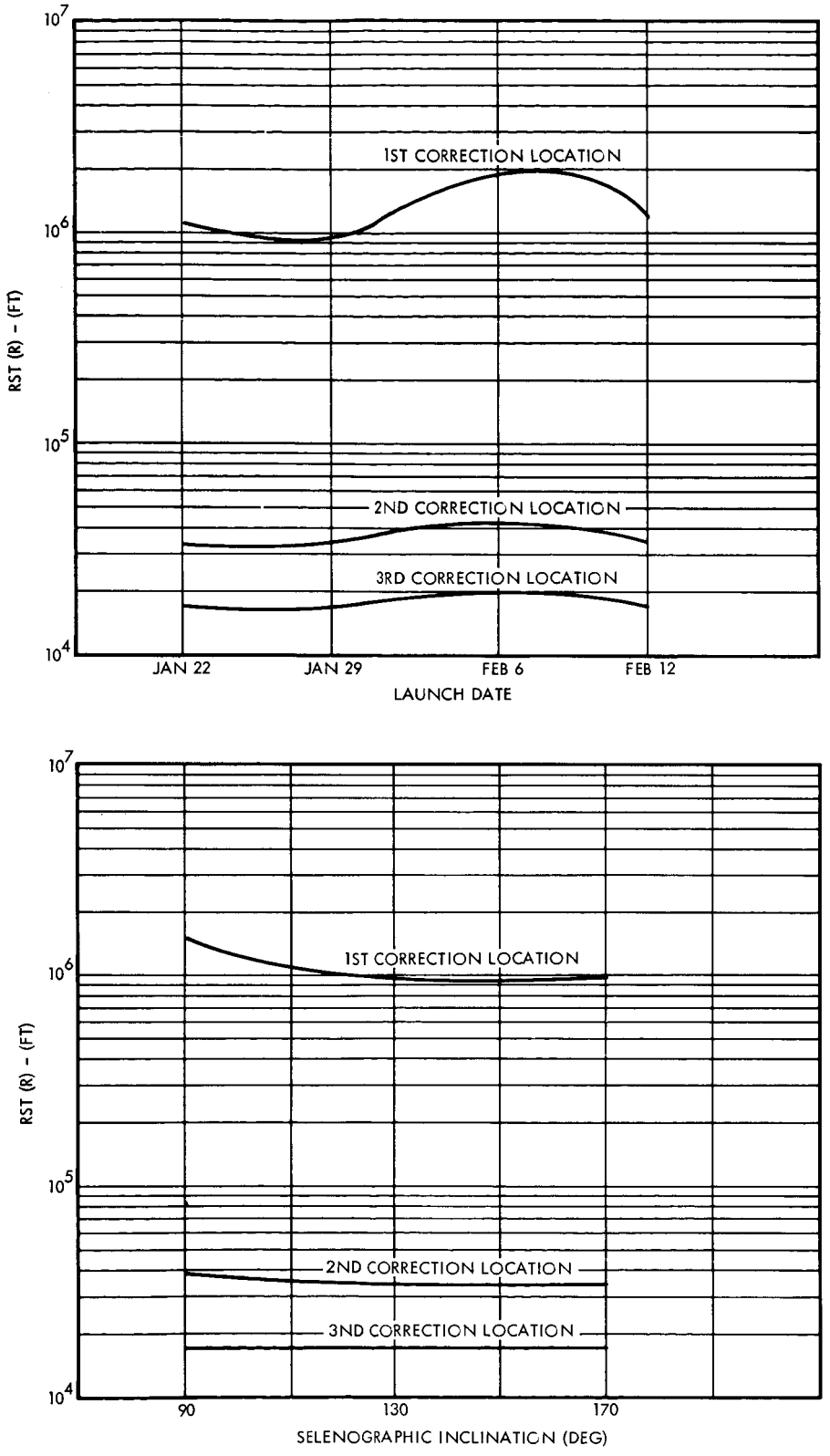

Figure 6.2.2-4. Effects of Date of Launch and Selenographic Inclination on Orbit Determination Using Optical Data

Uncertainties in position at lunar arrival as a function of time from injection are presented in Figure 6.2.2-5 for Group I, Group II (with range data), Group II (without range data), optical tracking, and the combination of Group II (without range data) and optical. Data are presented only for position, since velocity uncertainties behave in a similar manner. RST(R) is presented for Group I as a point at the time tracking ceases due to the vehicle exceeding the maximum range of the network at this time. Group II (with range data) is characterized by several sharp reductions in RST(R) within periods of one hour. This phenomenon occurs at the times when two stations are tracking the spacecraft simultaneously and is the result of the triangulation effect discussed in Section 6.3.1. The Group III network has been found to lead to uncertainties comparable to those of Group II. It may be noticed that there are periods during the flight, lasting for as long as ten hours, when there is relatively little improvement in tracking uncertainties from Group II data. During these periods it would be possible to reduce the sampling frequency without significantly affecting the overall tracking accuracy. The largest uncertainties from optical data are greater than those associated with DSIF (with range data) by as much as a factor of 50. Thus, the combination of optical and DSIF data, when range information is present, is not significantly better than DSIF data alone.

Tables 6.2.2-I and 6.2.2-II represent uncertainties remaining after tracking the spacecraft over a free-return trajectory to lunar arrival. These numbers are representative since tracking accuracy with this amount of data is insensitive to trajectory variations. Table 6.2.2-I presents these uncertainties in the form of RST(R) and RST(V) propagated to the nominal lunar arrival time, both with and without the effects of midcourse corrections. Table 6.2.2-II presents these uncertainties for DSIF (with range data) and optical tracking after propagation over a free-return trajectory to the nominal reentry altitude of 400,000 feet.

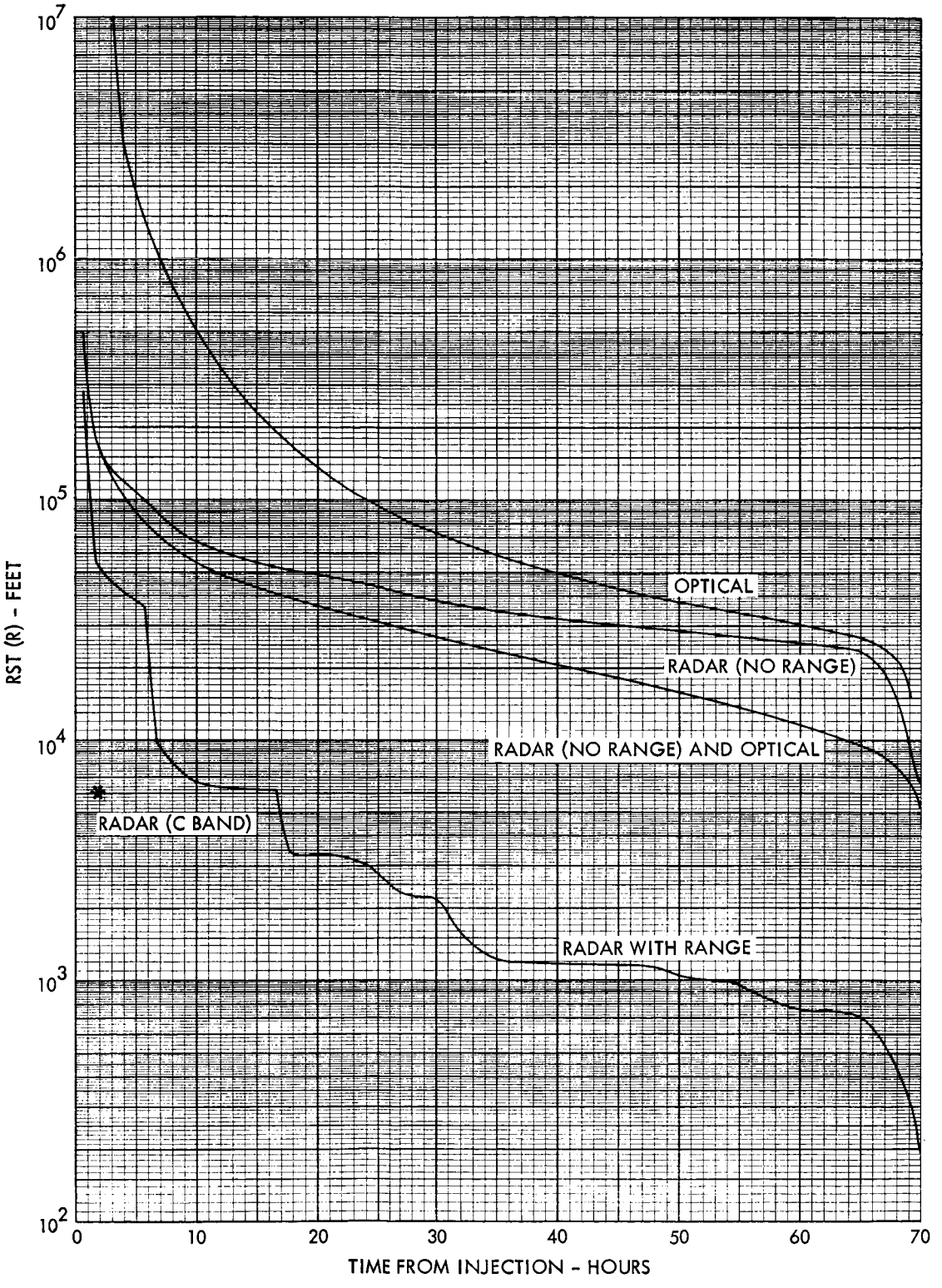

Figure 6.2.2-5. Comparison of Tracking Uncertainties Versus Data Types

Table 6.2.2-I. Lunar Arrival Uncertainties After Tracking to Lunar Arrival

Data Type	No Midcourse Corrections		With Midcourse Corrections	
	1σ Position Uncertainty (feet)	1σ Velocity Uncertainty (feet/sec)	1σ Position Uncertainty (feet)	1σ Velocity Uncertainty (feet/sec)
DSIF (Range)	250	0.20	2,500	1.50
DSIF (No Range) and Optical	6,200	3.10	9,200	5.60
DSIF (No Range)	6,800	5.10	12,300	9.60
Optical	17,500	9.00	28,000	16.00
C-Band Radar	6,200	1.20	--	--

Table 6.2.2-II. Reentry Uncertainties — No Midcourse Corrections

Data Type	1σ Flight Path Angle Uncertainty (degrees)	1σ Arrival Time Uncertainty (seconds)	1σ Velocity Magnitude Uncertainty (feet/seconds)
DSIF (With Range Data)	0.04	0.7	1.6
Optical	0.85	17.6	38.7

6.2.3 Lunar Parking Orbit

The lunar parking orbit phase of the Apollo mission begins at deboost of the spacecraft into a circular orbit about the moon and ends at injection of the CSM into a transearth return trajectory. During this period the LEM separates from the CSM vehicle and performs its powered flight and coast operations (descent to the surface and ascent to rendezvous). The CSM remains in its parking orbit during the entire phase which typically lasts a day or more. However, since the LEM operations are generally scheduled to begin after only a few revolutions in the parking orbit, the position and velocity of the spacecraft must be determined with a required accuracy as soon as possible after parking orbit injection. Thus, the orbit determination problem which is treated in this section is one of estimating the orbit uncertainties as a function of time based upon observations obtained in a given tracking interval initiated at parking orbit injection.

The parking orbit is designed to pass over a preselected lunar landing site, so that all the descent operations of the LEM will be in-plane. The selection of a particular combination of CSM orbit inclination and node which satisfies this constraint follows from a consideration of the hyperbolic approach geometry and the spacecraft plane change and deboost capability. Application of typical Apollo mission selection criteria results in retrograde, near-equatorial parking orbits. The combinations of the geometrical orbital elements selected for this analysis (i = 90, 130, 170 degrees; Ω = 0, 315, 270 degrees) include the typical case as well as some interesting special cases, such as the polar orbits with the line of nodes both parallel and normal to the direction of the earth. The tracking results are presented in terms of these elements which are measured in a selenographic coordinate system, with the ascending node referenced to the mean earth-moon line (positive eastward) and the inclination referenced to the moon's equator.

The conical elements selected (semi-major axis and eccentricity) are representative of Apollo missions in that the pericynthion altitude varies from 40 to 160 nautical miles in combination with eccentricities of 0.001 and 0.02, with the near-circular 80 nautical mile orbit designated the nominal case. In

this range of values the orbital period varies from 115.5 to 141.5 minutes with a nominal value of 122.5 minutes. Results presented in terms of these conical elements take into account this period variation.

The values of the final two elements, which complete the set of trajectory parameters required to completely define the initial state vector of the spacecraft,have been assumed and are held invariant throughout the analysis. The argument of pericynthion (180 degrees) and true anomaly at epoch (0 degrees) define the initial in-plane position of the spacecraft. Hence, the spacecraft is always injected at the equator, and its initial angular position with respect to the earth-based radar stations depends upon the location of the line of nodes.

For a given parking orbit, results are investigated for two particular dates — January 27 and February 10, 1968 — corresponding to southern and northern lunistice, respectively. The duration of the tracking interval is given discrete values of 1 and 2 complete orbital revolutions. These intervals are, in all cases, initiated at epoch (parking orbit injection); and the selection of this time in conjunction with the rotational orientation of the earth determines the visibility of the spacecraft from the earth-based radar stations. This point is best illustrated with the aid of Figure 6.2.3-1. On either date we have the choice of selecting the radar station grouping (DSIF Groups II or III) and the epoch. For example, on February 10 (positive lunar declination), with a selection of Group II and an epoch at midnight, both Madrid and Goldstone (northern hemisphere stations) have visibility, whereas with Group III, only Goldstone can view the spacecraft. Consideration is also given to the geographic locations of the stations. Hence, on January 27 (negative lunar declination), with a selection of Group III and an epoch at 2 hours, both Canberra and Johannesburg (southern hemisphere stations) have visibility. This case is effectively equivalent to the first case described above. Since the tracking interval has a maximum duration of approximately 4 hours (two revolutions prior to LEM separation), the epoch can be selected so as to constrain the number of tracking stations (either 1 or 2) which have visibility. Exemplary tracking results are generated primarily for an epoch at midnight on February 10 in conjunction with different combinations of tracking intervals and radar station groupings.

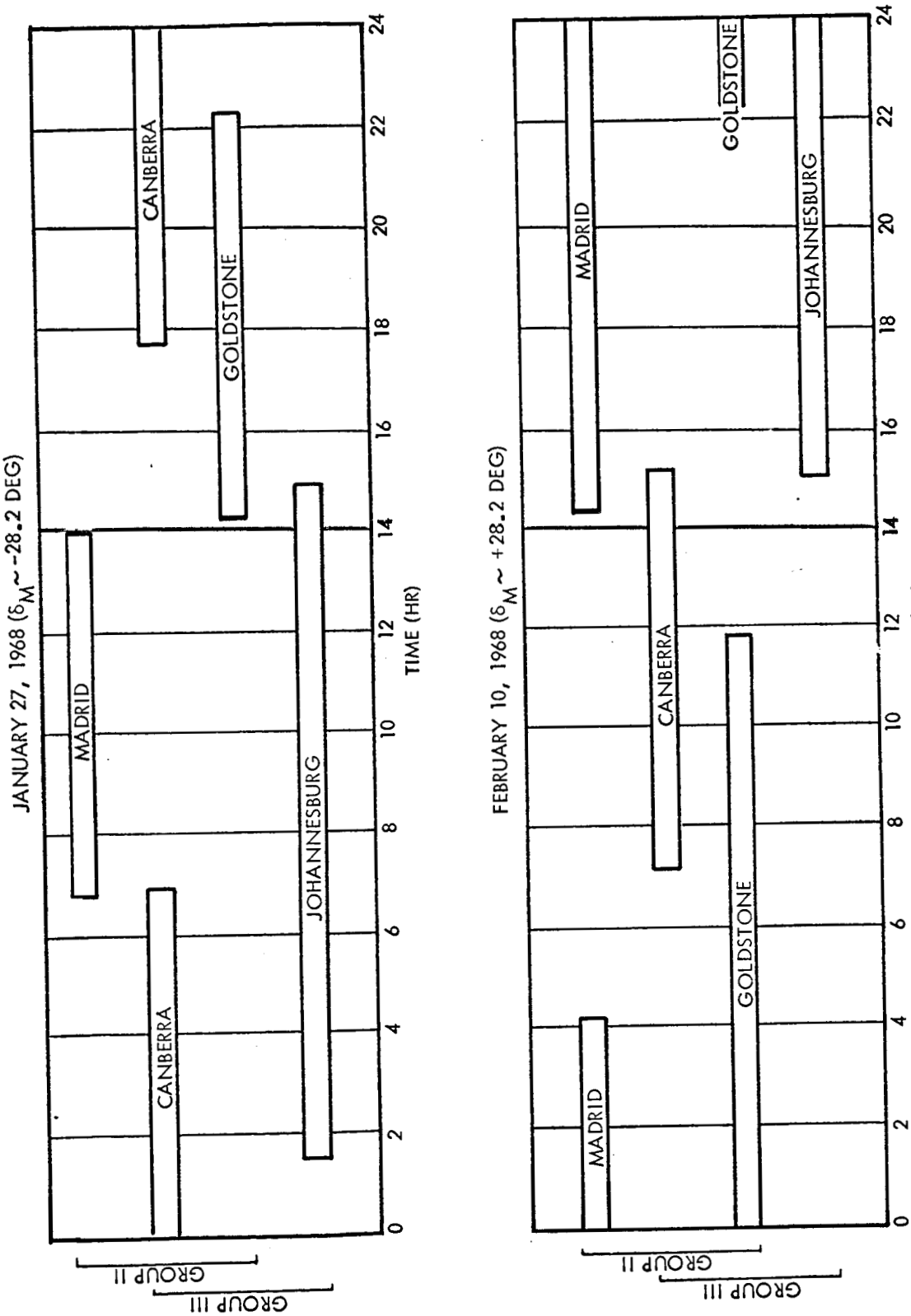

Figure 6.2.3-1. Visibility of Moon From DSIF Stations (Minimum Elevation Angle = 5°)

The radar tracking system uses simultaneous observations of range, azimuth, elevation, and range rate subject only to random noise. Furthermore, it is assumed that when visibility permits, two stations can track the spacecraft simultaneously; this leads to the advantageous triangulation effect. In addition, the tracking simulation assumes radar data dropouts during those periods when the spacecraft is eclipsed by the moon. By contrast, the tracking simulation with the optical system is continuous. Further information pertaining to these tracking systems and their operating characteristics can be found in Reference 1.

From the assumed times of tracking observations and sensor noise models the tracking program generates a covariance matrix of orbit uncertainties at epoch, measured in three different coordinate systems. No a priori information is assumed. These uncertainties are then propagated forward in time to the end of the third orbital revolution. Figure 6.2.3-2 represents the relationship between the true instantaneous orbit plane and that predicted from the tracking data. The orbit uncertainties propagated to a particular point in time are depicted in the orbit plane (radial, downrange, crossrange) coordinate system. The square roots of the mean square magnitudes of the position and velocity uncertainties designated RST(R) and RST(V), are used to indicate the bounds on the orbit uncertainties and serve as a basis of comparison of the results which follow.

Certain functional relationships exist among the uncertainties in orbit plane components. For example, the crossrange position and velocity are related geometrically such that a maximum uncertainty in one is accompanied by a minimum uncertainty in the other. The radial position and downrange velocity uncertainties, together with the correlations between these errors, indicate how well the orbital energy and angular momentum can be determined. Furthermore, an uncertainty in determining the in-plane position of the spacecraft with respect to pericynthion produces an uncertainty in radial velocity. Results in terms of these components are presented as additional information for the evaluation of the orbit determination accuracy.

Table 6.2.3-I summarizes the results for radar tracking only as a function of tracking interval and number of radar stations. For each combination of these parameters, the results are presented in terms of lunar geometry, and both the best and worst cases are given to indicate the range in uncertainties.

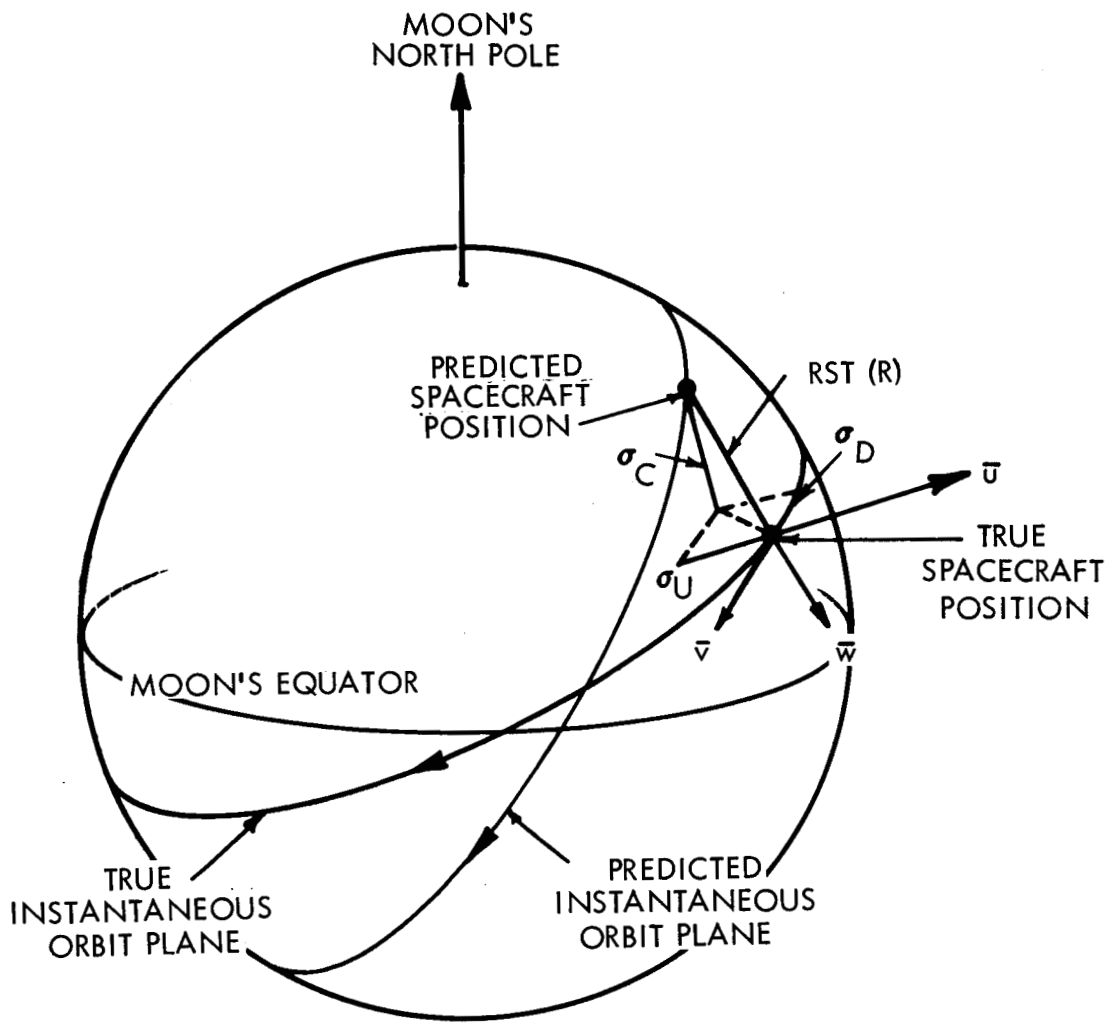

Figure 6.2.3-2. Orbit Uncertainties in $\vec{u}$, $\vec{v}$, $\vec{w}$ Coordinates

Table 6.2.3-I. Radar Tracking Only Propagated into Revolution Following Tracking

Tracking Interval* (revolutions)	Number of Observing Stations**		Maximum RST(R) (feet)	Maximum RST(V) (feet/sec)	Comments on Lunar Orbit Geometry	1σ Period Uncertainty (seconds)
2	2	Worst	< 6,000	< 5	Near-Equatorial	$0.004<\sigma_p<0.027$
		Best	< 1,200	< 1	Polar	
2	1	Worst	<38,000	<32	Polar, Ω = 0 degrees	$0.007<\sigma_p<0.089$
		Best	< 2,000	< 2	Polar, Ω = 270 degrees	
1	2	Worst	<17,000	<15	Near-Equatorial	$0.012<\sigma_p<0.449$
		Best	< 2,000	< 2	Polar	

* Starting at epoch
** Station Latitude corresponds to lunar declination

Table 6.2.3-II. Radar In-Plane Uncertainties Propagated into Revolution Following Tracking

Tracking Interval (revolutions)	Number of Observing Stations	Downrange		Radial	
		σ_D(feet)	$\dot{\sigma}_D$(feet/sec)	σ_u(feet)	$\sigma_{\dot{u}}$(feet/sec)
2	2	<900	<0.03	< 40	<0.80
2	1	<2900	<0.04	< 70	<2.50
1	2	<6100	<0.40	<600	<5.20

Notice that in the case of simultaneous observations from two radar stations, the orbit uncertainties tend to be the largest for the near-equatorial geometry. In the cases where only one station is tracking, the uncertainties are consistently large except when the orbit plane is normal to the radar line-of-sight (i = 90 degrees; Ω = 270 degrees). However, the uncertainties for near-equatorial orbits become as large as 26,000 feet in position and 22 feet per second in velocity. The orbital period uncertainties reflect the knowledge of the in-plane components. Except for the 1-revolution case, the period can be determined to less than 100 milliseconds. In most cases the crossrange uncertainties predominate, and as a result, the propagated RST uncertainties display significant periodic (1/2 rev) fluctuations and correspondingly small secular increases. Table 6.2.3-II summarizes the radial and downrange uncertainties for the same cases presented above.

Typically, for radar tracking only, the total propagated uncertainties in position and velocity are minimized when two stations are in a position to make observations during the entire tracking interval (subject only to data dropouts during eclipse periods). If one of the stations should cease tracking, say, half way through the interval (due, for example, to equipment failure or loss of visibility), some increase in the uncertainties can be expected — perhaps 25 percent. However, if one of the stations is dropped altogether, the uncertainties would increase by approximately a factor of 4. This indicates the importance of making observations from two different earth-based stations, either simultaneously or sequentially, during the tracking interval.

It was found that RST(R) and RST(V) decrease with increasing altitude and eccentricity in the range of values investigated, owing mainly to the increasing orbital period and tracking time on any given pass. For example, RST(R,V) at 160 nautical miles is approximately one-half RST(R,V) at 40 nautical miles. But this does not seem to be an extremely significant effect in view of the fact that these particular trajectory parameters are fairly well constrained by other mission considerations.

The orbit uncertainties also decrease with increasing data rates according to the equation

$$RST'(R,V) \sim \sqrt{\frac{\dot{D}}{\dot{D}'}}\ RST(R,V) \quad ,$$

where the data rates, $\dot{D}$ and $\dot{D}'$, have values in the range 0.25 to 2.0 samples per minute. This permits the given results to be scaled for departures from the nominal radar characteristics of 0.5 samples per minute.

Finally, it should be pointed out that the radar results are dominated by the range measurement, with a 1σ random error of 100 feet. If the range measurement is deleted, the orbit uncertainties increase by approximately a factor of 4. The effect is much the same if the range measurement is retained but the 1σ error is increased to 1,000 feet. For range rate only, the uncertainties are greater by approximately a factor of 5.

For optical tracking only, the results are independent of lunar geometry and the selection of epoch. As a result the conclusions can be more definitive in that the tracking interval becomes the primary study parameter, an increase of which leads to reduced orbit uncertainties. Results for tracking intervals of 1- and 2-orbital revolutions are presented in Table 6.2.3-III. Notice that the period uncertainties are larger than in the case of radar only, while the cross-range uncertainties are smaller. This indicates that the propagated uncertainties are dominated by the in-plane components (downrange position and radial velocity in particular) which exhibit significant secular increases with time. Hence, uncertainties propagated much beyond the third revolution would become significantly large; but up to that point, the optical system offers the better estimate of the parking orbit.

When the two tracking systems are combined, best features of each tend to complement each other; that is to say, the radar determines the in-plane orbit components with sufficient accuracy while the optical does well in determining the crossrange components. Table 6.2.3-IV summarizes the results for the combined tracking, and points out the fact that the effect of lunar geometry and epoch have been minimized with the addition of optical data, and that the

Table 6.2.3-III. Optical Tracking Only

Tracking Interval (revolutions)	Maximum RST(R) (feet)	Maximum RST(V) (feet/sec)	1σ Period Uncertainty (seconds)	Crossrange Uncertainties	
				σ_c(feet)	$\sigma_{\dot{c}}$(feet/sec)
1	<10,000	<9.0	0.75	<1,200	<1.10
2	< 3,000	<2.5	0.21	< 900	<0.75

Table 6.2.3-IV. Combined Radar and Optical Tracking

Tracking Interval (revolutions)	Number of Observing Stations	Maximum RST(R) (feet)	Maximum RST(V) (feet/sec)	1σ Period Uncertainty (seconds)
1	1	<6,000	<5.5	$0.016 < \sigma_p < 0.477$
2	2	< 900	<0.75	~ 0.004

primary considerations for orbit determination are the length of the tracking interval and the number of earth-based radar stations making observations. The effect of radar data loss from one of two stations is not as significant as long as the optical data is maintained, but the orbit uncertainties can more than double if radar data are lost altogether. The dependency upon the optical data is more pronounced as can be seen by comparing the results. Of course, these conclusions are based upon the assumption that the optical data rate can be maintained continuously throughout the tracking interval.

6.2.4 Transearth Trajectory

It is the purpose of this section to illustrate those uncertainties in reentry conditions due to tracking of transearth trajectories, which could reasonably exist over a range of important orbital parameters and tracking network characteristics.

The principal coordinate system considered is the polar reentry coordinate system, illustrated in Figure 6.2.4-1. At reentry the estimated parameters are longitude (λ), latitude (ϕ), flight path angle (β), azimuth (A), geocentric distance (r), and velocity magnitude (V). For this analysis, reentry altitude is fixed at 400,000 feet above the earth's surface and uncertainties in β are measured at this altitude, thus defining an entry corridor. However, since reentry altitude is taken as fixed, the geocentric distance parameter (r) is not variable and is replaced by time-of-flight to the fixed reentry altitude. Therefore, the six parameters of the polar reentry coordinate system are λ, ϕ, β, A, V and time-of-flight (t) to the fixed reentry altitude. Since errors in λ, ϕ, and A are small and not critical to effecting a safe reentry, uncertainties in β, V, and t are stressed in evaluating variations in the important orbital parameters and tracking network characteristics.

Typical uncertainties at reentry in flight path angle (β), velocity (V), and time of arrival (t) as a function of time from injection as a result of employing onboard optical tracking only, over a nominal 75-hour trajectory are presented in Figure 6.2.4-2. In Figure 6.2.4-3, the same trajectory as illustrated in Figure 6.2.4-2 was investigated for: Group II and Group III earth-based radar tracking with range, range-rate, azimuth, and elevation data types. When all radar stations and data types are combined, sharp drops in predicted uncertainties are noted in their histories. These decreases are associated with the times at which the spacecraft becomes visible to a different tracking station. At these times, data taken by the second station provides position and velocity information in a direction where larger uncertainties previously existed. This effect, termed triangulation(discussed in section 6.3.1) results in a pronounced improvement in the predicted uncertainties when range data are employed due to the relatively small errors with which range measurements can be taken. Without range data, the improvement in predicted uncertainties is considerably less

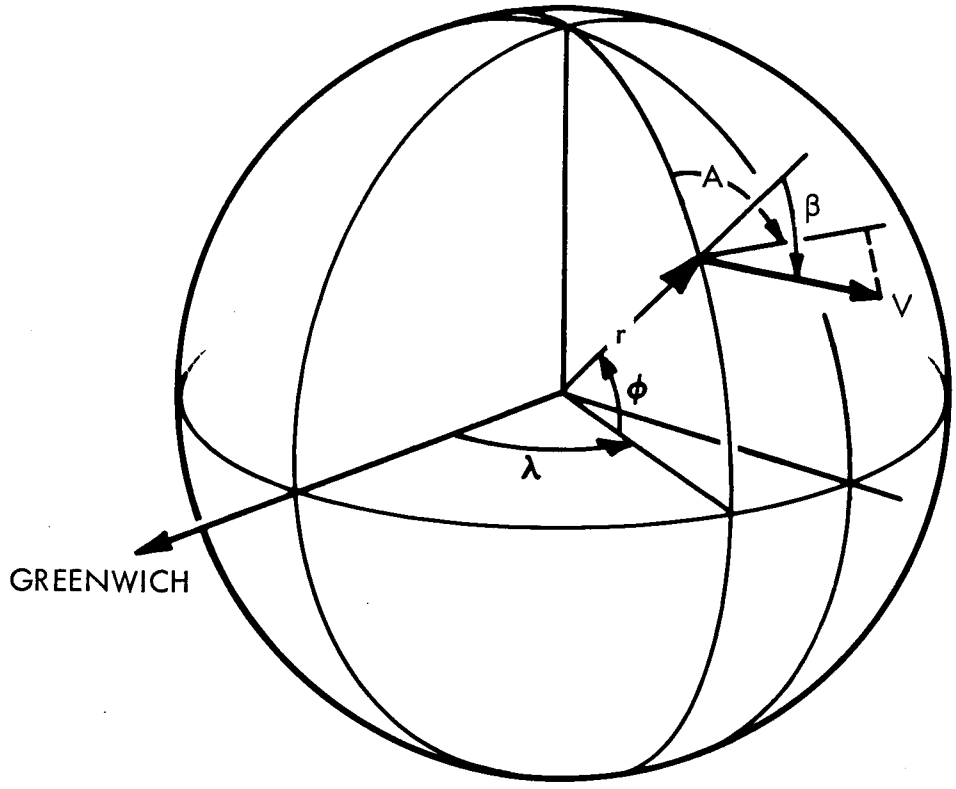

Figure 6.2.4-1. Polar Reentry Coordinate System

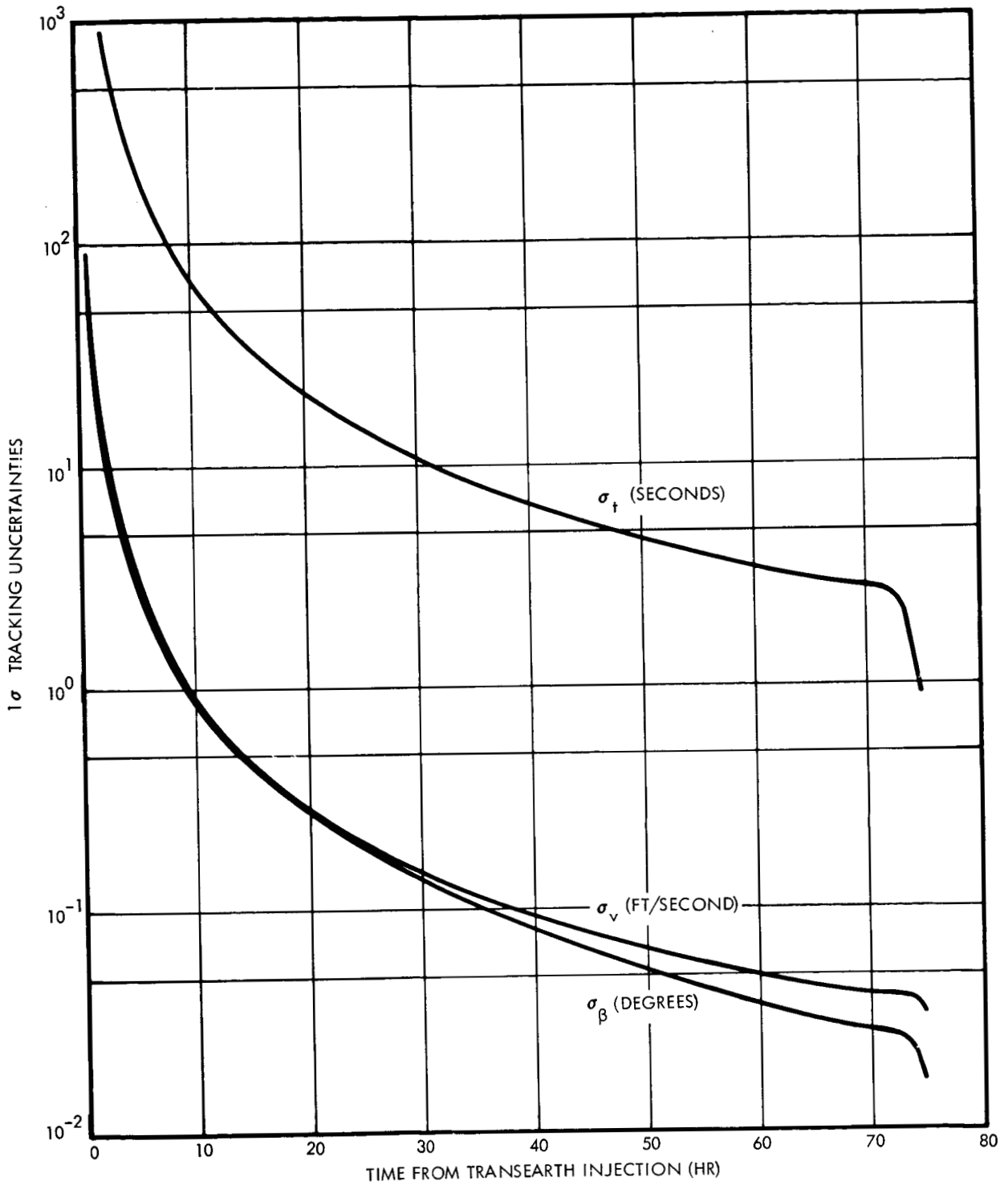

Figure 6.2.4-2. Typical β, V, t Reentry Uncertainty Profiles as a Function of Transit Time

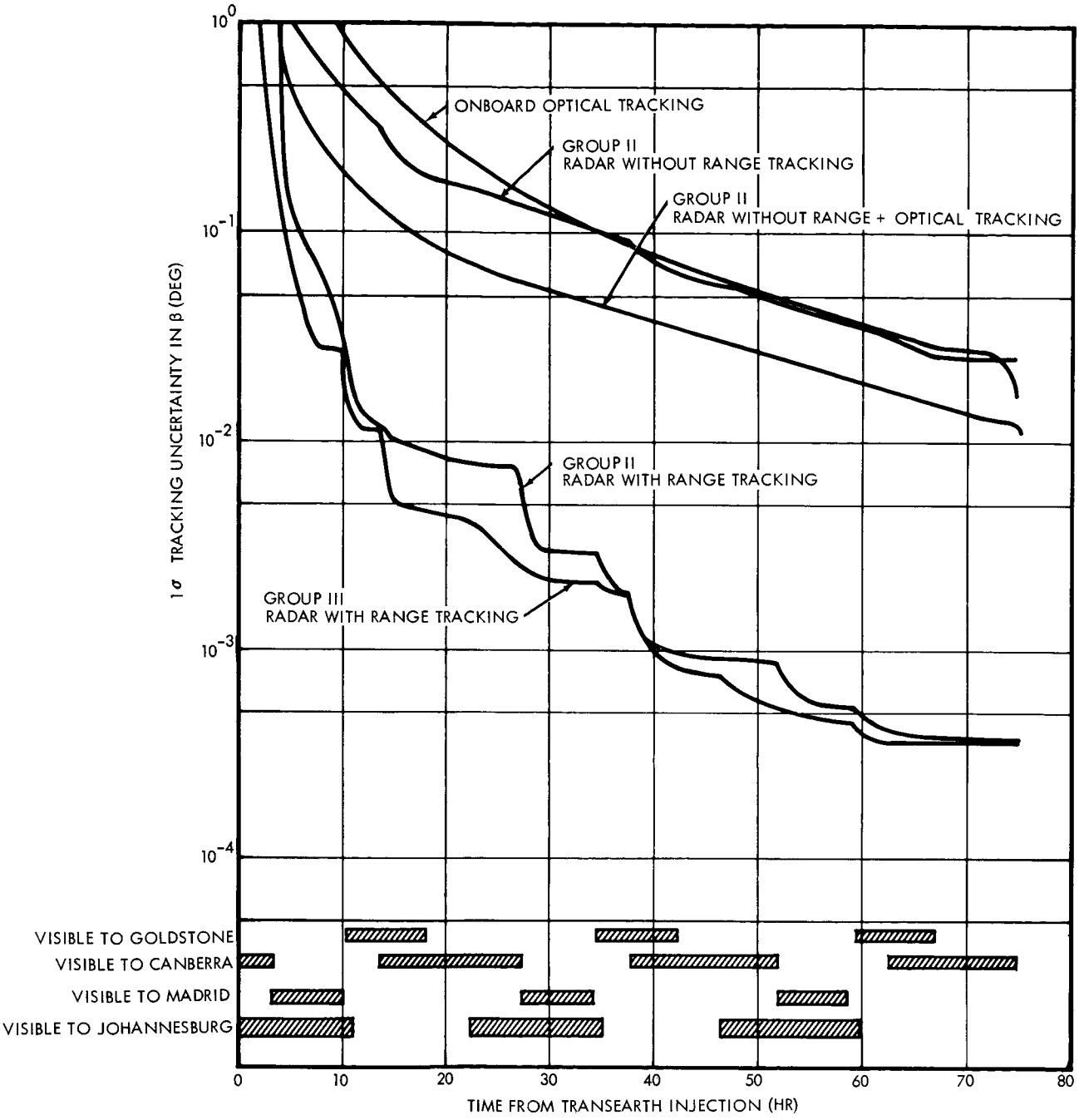

Figure 6.2.4-3. Effect of Changing Tracking Data Type on Uncertainties at Reentry

pronounced due to the relatively large errors associated with the angular measurements. A secondary effect, associated with the times during which the spacecraft is visible to more than one station, results simply from an increase in available data. Also to be noted from Figure 6.2.4-3, when range data is not available and only range rate, azimuth, and elevation data types combined, the predicted uncertainty in β is degraded by approximately two orders of magnitude.

For the optical tracking mode, the slopes of the uncertainty profiles are steeper near the beginning and end of the trajectory. This is due to the relative nearness of the spacecraft to the observed bodies and is also a function of the curvature of the trajectory near the observed body. With landmark uncertainties of the assumed size and a sextant accuracy of the assumed level, the landmark error dominates the optical sightings for the first three to four hours following transearth injection and preceding atmospheric reentry, while the sextant error in sighting the landmark dominates during the remaining portion of the return trajectory until very near reentry. If onboard optical information is combined with earth-based radar information consisting of range, range rate, azimuth and elevation data, no noticeable improvement is gained over using radar data alone. A combination of optical and radar without range data, however, takes advantage of the best features of each, yielding the lower uncertainties during the early portion of the trajectory due to DSIF information and an improvement near the end of the trajectory due to an improvement in optical sightings near the earth. It is important to note in Figure 6.2.4-3 that although the combined tracking system improves the predicted uncertainties by as much as a factor of 10 during the early portion of the trajectory, the uncertainties near the end are similar to those uncertainties obtained by optical or radar without range tracking alone.

The influence of the trajectory parameters in determining the transearth orbit using ground-based radar tracking or onboard optical tracking is reflected in Tables 6.2.4-I and 6.2.4-II respectively. When radar is employed, the accuracy to which an orbit can be determined is strongly dependent upon the tracking visibility for the various stations and the tracking geometry. Thus, when evaluating the uncertainties at reentry due to radar tracking in terms of transearth trajectory characteristics, it must be remembered that these characteristics

Table 6.2.4-I. 1σ Uncertainties at Reentry in β, V, t as a Function of the Trajectory Parameters Using Group II Radar Information with Range, Range Rate, Azimuth and Elevation Data Types, and No Midcourse Corrections

Trajectory No.	Lunar Declination (deg)	Trajectory-Plane Inclination (deg)	Landing Site	Flight Time (hr)	1σ Uncertainties at Reentry		
					β (deg)	V(ft/sec)	t(sec)
1	+28 (max)	30	San Antonio	60	1.59×10^{-4}	7.45×10^{-5}	4.39×10^{-3}
2	+28	30	San Antonio	75	3.71×10^{-4}	11.4×10^{-5}	13.5×10^{-3}
3	+28	30	San Antonio	90	9.59×10^{-5}	5.51×10^{-5}	2.87×10^{-3}
4	+28	40	San Antonio	60	1.19×10^{-4}	6.64×10^{-5}	3.27×10^{-3}
5	+28	50	San Antonio	60	1.25×10^{-4}	1.31×10^{-5}	3.43×10^{-3}
6	0 (null)	30	San Antonio	60	2.73×10^{-4}	1.17×10^{-5}	8.02×10^{-3}
7	0	30	Woomera	60	1.34×10^{-4}	9.41×10^{-6}	3.89×10^{-3}
8	-28 (min)	30	Woomera	60	1.42×10^{-4}	7.85×10^{-5}	4.11×10^{-3}

Table 6.2.4-II. 1σ Uncertainties at Reentry in β, V, t as a Function of the Trajectory Parameter Using Onboard Optical Measurements and No Midcourse Corrections

Trajectory No.	Lunar Declination (deg)	Trajectory-Plane Inclination (deg)	Landing Site	Flight Time (hr)	1σ Uncertainties at Reentry		
					β (deg)	V(ft/sec)	t(sec)
1	+28 (max)	30	San Antonio	60	2.08×10^{-2}	4.66×10^{-2}	1.01×10^{0}
2	+28	30	San Antonio	75	1.68×10^{-2}	3.41×10^{-2}	9.09×10^{-1}
3	+28	30	San Antonio	90	1.49×10^{-2}	3.37×10^{-2}	8.45×10^{-1}
4	+28	40	San Antonio	60	2.04×10^{-2}	4.22×10^{-2}	1.00×10^{0}
5	+28	50	San Antonio	60	2.02×10^{-2}	3.88×10^{-2}	9.72×10^{-1}
6	0 (null)	30	San Antonio	60	2.10×10^{-2}	0.673×10^{-2}	9.89×10^{-1}
7	0	30	Woomera	60	2.22×10^{-2}	0.587×10^{-2}	1.06×10^{0}
8	-28	30	Woomera	60	2.18×10^{-2}	4.27×10^{-2}	1.05×10^{0}

must in turn be evaluated in terms of their effect on the tracking situation. For example, the uncertainty in β between trajectory No. 6 and trajectory No. 7 in Table 6.2.4-I differs by approximately a factor of two. From the standpoint of trajectory parameters, the only difference between trajectory No. 6 and trajectory No. 7 is the landing site selection, implying a factor of two degradation in the knowledge of β for choosing San Antonio, Texas as the targeting point over Woomera, Australia. Such, however, is not the case from a tracking standpoint. Transearth trajectory No. 6 injects out of lunar orbit at a different Julian time than trajectory No. 7. Hence, earth-based tracking is initiated by different stations in the selected tracking group due to the fact that the earth is in a different position and station overlapping occurs in a different sequential order. Also, total overlapping station coverage, hence total data sampling, is greater for trajectory No. 7 than trajectory No. 6. It is therefore the effect of landing site selection on the tracking geometries that accounts for the factor of two degradation and not simply the difference in landing sites per se. Uncertainties in β, V, and t at reentry on the order of 10^{-4} degrees, 10^{-5} feet per second and 10^{-3} seconds, respectively, are noted for DSIF radar with range tracking over the variations in trajectory parameters investigated. The accuracy to which a transearth orbit can be determined using only onboard optical tracking is reflected in Table 6.2.4-II. In contrast to the radar tracking problem, the results for optical tracking are not appreciably influenced by the transearth orbit geometry. Consequently the tracking interval is the only major parameter that needs to be considered in evaluating the capability of the onboard optical tracker. For those trajectories with 60-hour flight times, 1σ uncertainties in β of approximately 0.002 degree at reentry result. If the flight time is increased to 75 and 90 hours the 1σ uncertainty in β drops to approximately 0.017 and 0.015 degree, respectively. Similar trends would also be apparent, however, if flight time was held constant and the sampling rates allowed to increase over a given trajectory.

Midcourse corrective impulses were simulated at 10 and 48 hours after injection and 2 hours prior to reentry for a typical transearth trajectory. Tracking through a midcourse maneuver was simulated by retaining the spacecraft position information in the three respective inertial Cartesian directions and degrading the velocity information by 0.1 meter per second, 1σ, in the remaining

three inertial velocity directions. The uncertainties at reentry in β are presented in Figure 6.2.4-4 for: Group II radar tracking with and without range information, onboard optical sightings, and onboard optical sightings combined with ground-based radar information without range. Following the three midcourse simulations, uncertainties in β at reentry are noted to be comparable for the several tracking schemes. If C-band (Group I) radar is employed in addition to the nominal tracking scheme, following the third midcourse correction, uncertainties at reentry then become comparable to those cases where no midcourses were applied and DISF radar tracking with range was employed.

In summary, Table 6.2.4-III presents the 1σ uncertainties in flight path angle (β), velocity (V) and time of arrival (t) at reentry with and without the effects of midcourse corrections. Values presented are measured at reentry for a typical trajectory.

Feb-Out #1

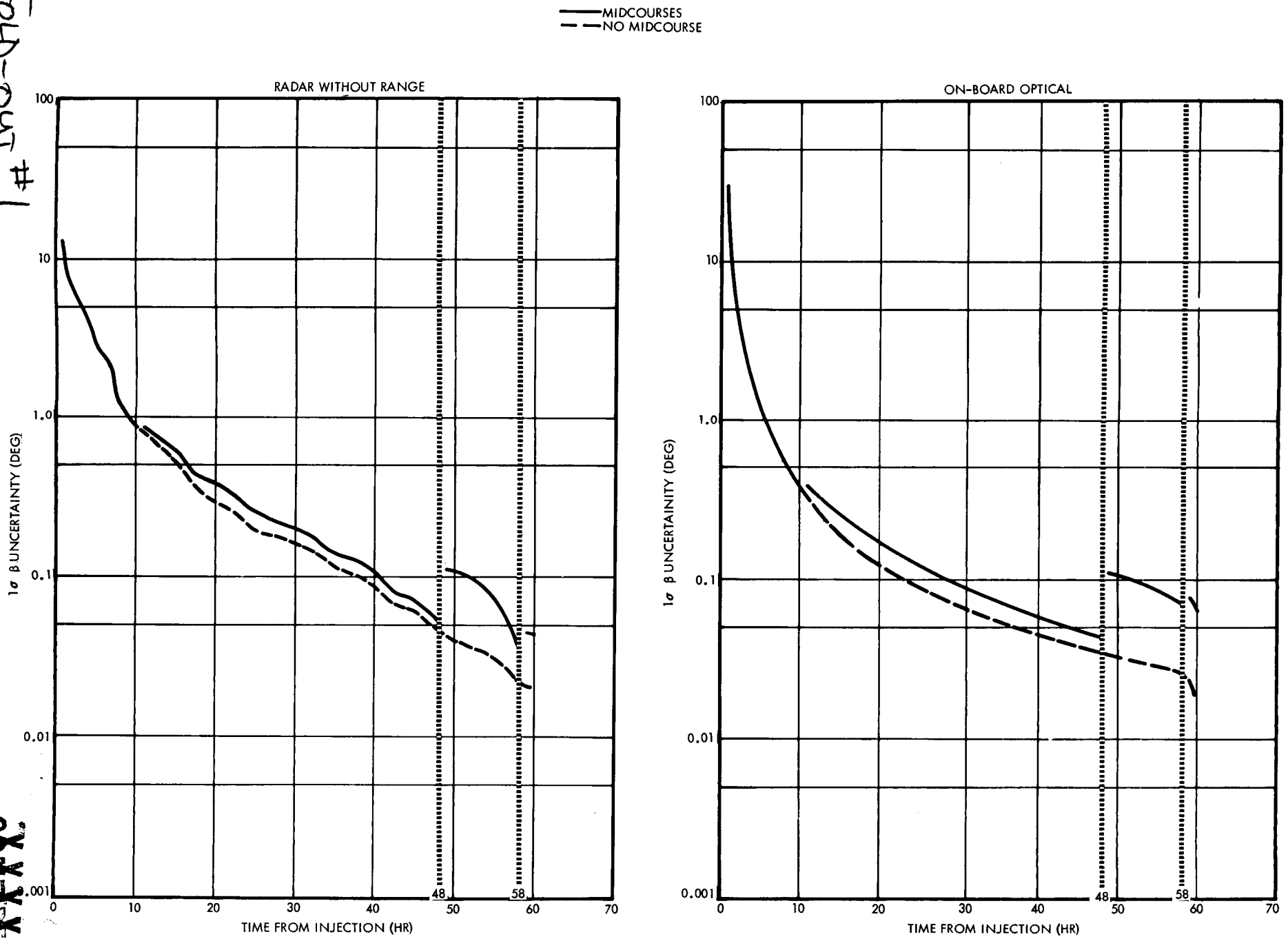
MIDCOURSES
NO MIDCOURSE
RADAR WITHOUT RANGE
ON-BOARD OPTICAL
1σ β UNCERTAINTY (DEG)
100
10
1.0
0.1
0.01
.001
0.001
0
10
20
30
40
48
50
58
60
70
TIME FROM INJECTION (HR)

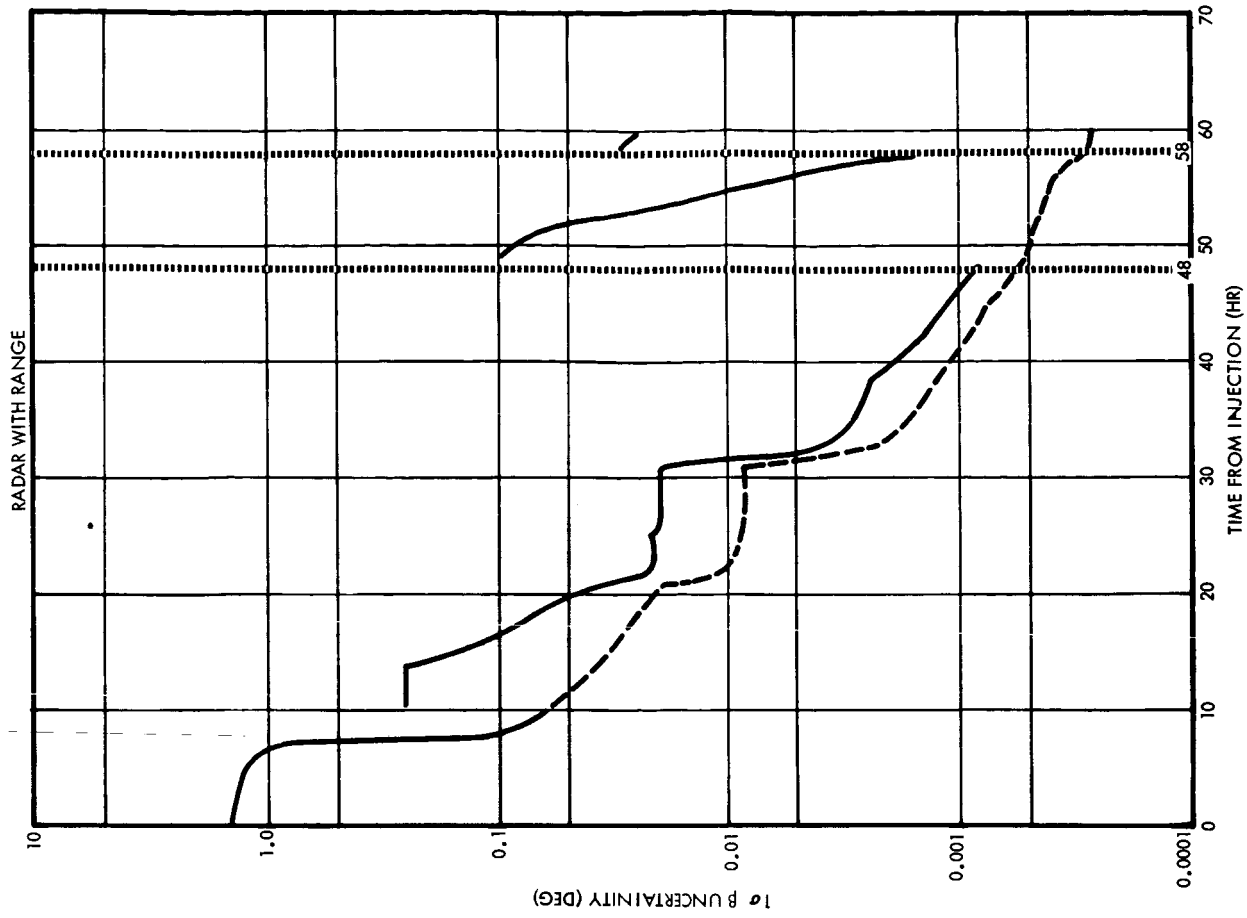

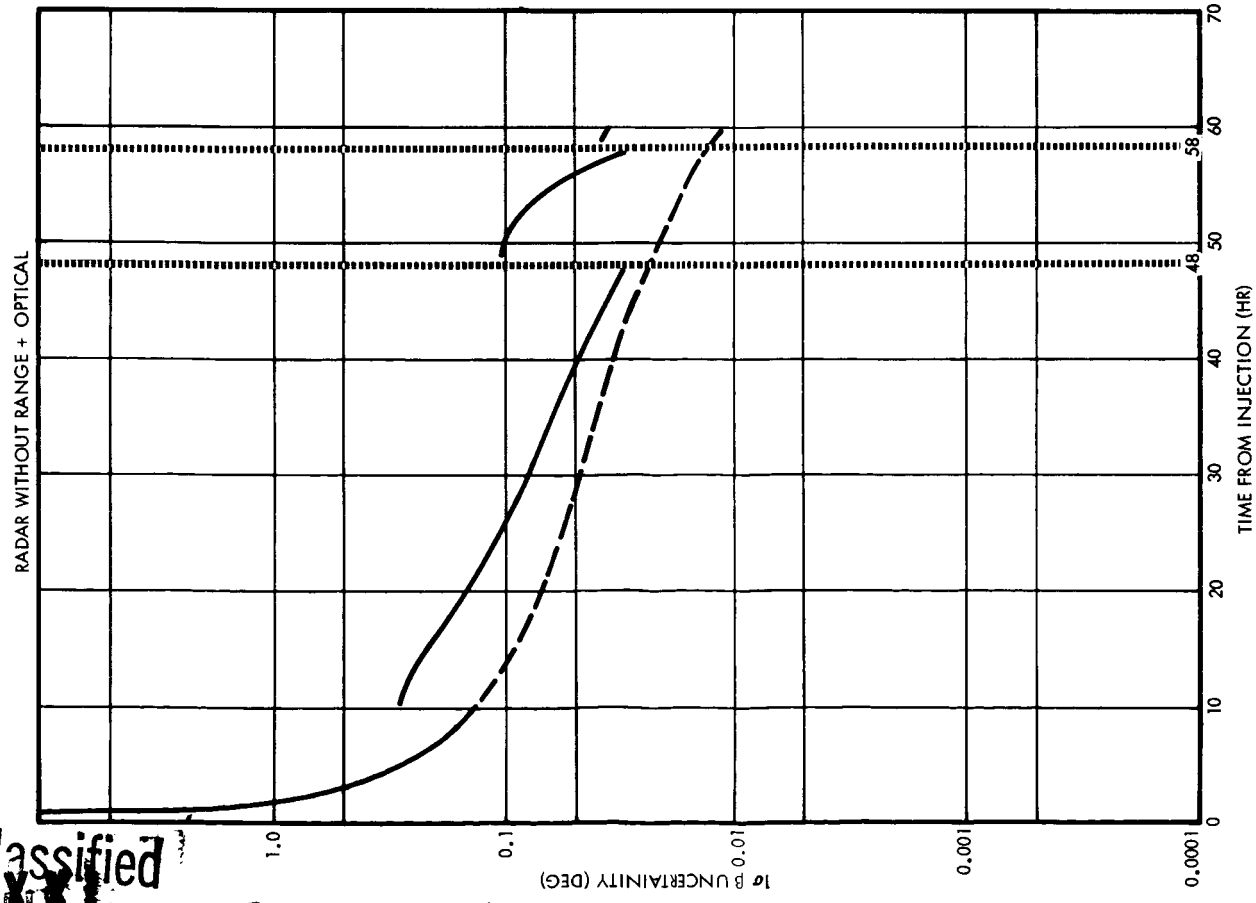

Figure 6.2.4-4. The Effect of Midcourse Corrections on Reentry Uncertainty

FOLD-OUT #2

Table 6.2.4-III. Transearth Tracking Summary

Data Type	Without Midcourse Corrections			With Midcourse Corrections		
	1 σβ (deg)	1 σV (ft/sec)	1 σt (sec)	1 σβ (deg)	1 σV (ft/sec)	1 σt (sec)
DSIF (range)	0.00027	0.000012	0.0080	0.0023	0.0053	0.24
DSIF (no range and optical)	0.011	0.0013	0.29	0.035	0.012	0.80
DSIF (no range)	0.021	0.0017	0.46	0.043	0.017	0.90
Optical	0.021	0.0067	1.0	0.062	0.080	2.1

6.3 COMMENTS

Some significant features of both radar and optical tracking are discussed in the following ~~four~~ THREE sections. For radar, the peculiar effects associated with simultaneous range measurements from two stations are described, and a theory is proposed in Section 6.3.1. The usefulness of optical tracking data in lunar missions is the subject of Section 6.3.2, and Section 6.3.3 suggests an approximate method of spacing optical observations to make the best use of their potential.

6.3.1 Range Triangulation Effects

In the translunar and transearth phases of this study, uncertainties in miss were plotted as functions of the amount of tracking time. The resulting curves for radar tracking with range data show peculiar, abrupt drops at several times. In order to explain these results, the theory of range triangulation has been proposed.

Examination of the drops in the uncertainty curves (see Sections 6.2.2 and 6.2.4) revealed that they always occurred when the visibility periods of two radar stations overlapped or almost overlapped. However, overlapping did not always produce an abrupt drop. If no midcourse corrections were simulated, the usual pattern consisted of three drops early in the trajectory and none thereafter. This indicated that the first overlapping of each pair of stations was significant, but that subsequent overlappings of the same stations were insignificant. If the effects of midcourse corrections were included, however, the pattern of drops changed. Prior to the first correction the pattern was the same, but after the corrections new drops appeared and old ones changed their sizes. This variation in the effects of overlapping coverage indicates that the results depend on the tracking history before the overlap occurs as well as the particular stations involved.

The use of the term triangulation in connection with overlapping tracking coverage comes from the fact that simultaneous range measurements from two stations determine two sides of a triangle with the spacecraft at one vertex and the stations at the other vertices. The third side is known from the station locations.

In order to understand the range triangulation theory, it is first necessary to recognize the fact that a single range measurement gives information about the position of the vehicle relative to the tracking station only along the topocentric radial direction. That is, the measurement may tell precisely how far away the vehicle is, but it tells nothing of the orientation of the orbit. The measurement also gives no indication of the relative velocity of the vehicle. Thus only one of the six parameters needed to determine the state of the vehicle is obtained from a single range measurement.

It might be assumed that the state vector would be uniquely defined as soon as six measurements had been made. If the six measurements were linearly independent this assumption would be valid. However, there is a tendency for the range measurements to be dependent.

In forming the least-squares estimate the partial derivatives of observations with respect to orbit parameters are used. The partials for one observation form a row in the A matrix, (see Reference 1) and the total differential of the observation can be computed by multiplying this row by a column consisting of differentials of the orbit parameters. That is,

$$A = \begin{bmatrix} \frac{\partial R_1}{\partial X} \\ \vdots \\ \frac{\partial R_i}{\partial X} \\ \vdots \\ \frac{\partial R_n}{\partial X} \end{bmatrix}$$

and $\delta R_i = \left| \partial R_i / \partial X \right| \delta X$

where X is the column vector of orbit parameters and R_i is the i-th observation. Therefore, $\left| \partial R_i / \partial X \right|^T$ is the gradient vector of the i-th observation.

The significance of the gradient vector to this discussion is that it indicates the direction of a differential in X which produces the maximum

differential in R_i (about the nominal point). In addition, differentials in X perpendicular to the gradient produce a zero differential in R_i.

In order to solve for the components of X which minimize the sum of squares of residuals, the gradient vectors of the observations must span the X space. This is simply another way of saying that $(A^T WA)^{-1}$ must exist. If the gradient vectors do not span the X space, then there is some direction in which X can be changed without changing any of the observations. Therefore, the observations can not measure deviations in that direction. Only the a priori information in this direction can be used. Similarly, if there is a direction for which all of the gradient vectors have only small components, the accuracy of measuring a deviation in X in that direction is not good (compared to the accuracy obtained in other directions). In tracking a translunar or transearth trajectory the components of the gradient vectors in some directions may be so small that they are made extremely uncertain by roundoff. When this happens numerical difficulties arise in calculating $(A^T WA)^{-1}$. When range measurements from only one station are used, such difficulties occur. The motion of the station improves the situation slightly, but simultaneous range measurements from two widely separated stations give a dramatic improvement. Simultaneous measurements from three stations should be even better, but this was impossible with the DSIF station locations used in this study.

Some insight can be obtained by considering the problem of measuring the position of the vehicle in the plane determined by it and two tracking stations. In the plane the geometry is as shown in Figure 6.3.1-1.

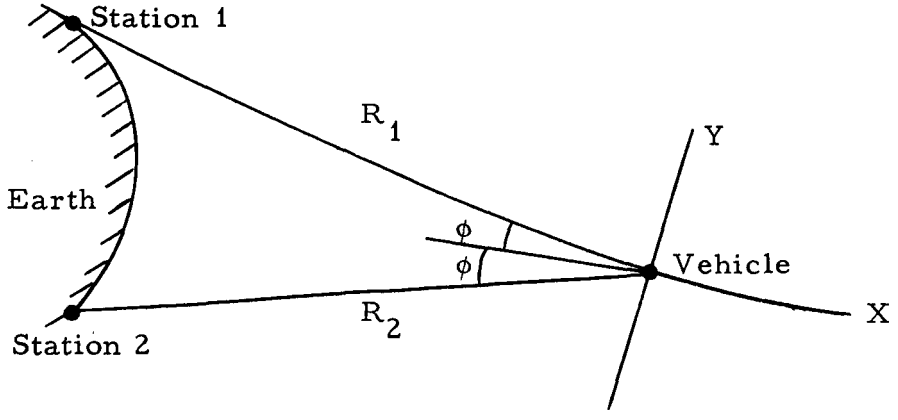

Figure 6.3.1-1

Unclassified
CONFIDENTIAL

Stations 1 and 2 measure ranges R_1 and R_2, respectively.

The gradient vectors ∇R_1 and ∇R_2 are shown in Figure 6.3.1-2.

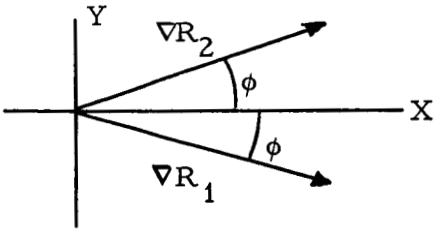

Figure 6.3.1-2

The components in the coordinate system shown are given by

$$\nabla R_1 = \begin{bmatrix} \cos\phi \\ -\sin\phi \end{bmatrix} \qquad \nabla R_2 = \begin{bmatrix} \cos\phi \\ \sin\phi \end{bmatrix}$$

and the partial derivative matrix is

$$A = \begin{bmatrix} \cos\phi & -\sin\phi \\ \cos\phi & \sin\phi \end{bmatrix}$$

The weighting matrix is

$$W = \begin{bmatrix} \frac{1}{\sigma^2} & 0 \\ 0 & \frac{1}{\sigma^2} \end{bmatrix}$$

where σ^2 is the variance of each range measurement.

The normal matrix is, therefore,

$$A^T W A = \begin{bmatrix} \cos\phi & \cos\phi \\ -\sin\phi & \sin\phi \end{bmatrix} \begin{bmatrix} \frac{1}{\sigma^2} & 0 \\ 0 & \frac{1}{\sigma^2} \end{bmatrix} \begin{bmatrix} \cos\phi & -\sin\phi \\ \cos\phi & \sin\phi \end{bmatrix}$$

$$A^T W A = \begin{bmatrix} \frac{2}{\sigma^2}\cos^2\phi & 0 \\ 0 & \frac{2}{\sigma^2}\sin^2\phi \end{bmatrix}$$

The covariance matrix of the error in measuring x and y with R_1 and R_2 is

$$(A^T W A)^{-1} = \begin{bmatrix} \frac{\sigma^2}{2\cos^2\phi} & 0 \\ 0 & \frac{\sigma^2}{2\sin^2\phi} \end{bmatrix}$$

and the standard deviations are

$$\sigma_x = \frac{\sigma}{\sqrt{2}\cos\phi} \qquad \sigma_y = \frac{\sigma}{\sqrt{2}\sin\phi}$$

If ϕ is small

$$\sigma_x = \frac{\sigma}{\sqrt{2}} \qquad \sigma_y = \frac{\sigma}{\sqrt{2}\,\phi}$$

If $\phi \to 0$, then $\sigma_y \to \infty$ and information is obtained only along the x direction. Therefore, it is desirable to keep ϕ as large as possible.

If the coordinates at the time of the measurement are not the parameters being estimated (as is usually the case), the plane referred to above corresponds to two-dimensional sub-space in the six-dimensional (if six parameters are used) parameter space. The particular sub-space depends on the locations of the two tracking stations involved.

A practical application of the theory of triangulation could be in the selection of new tracking station sites. Any additions or modifications in the DSIF network which might be considered for Apollo could be analyzed with respect to their effectiveness in producing triangulation. A simplified outline of such an analysis is included below.

If triangulation is to occur, there must be at least two stations in use. To be most effective, these should be placed approximately 180 degrees apart in longitude, with one at a north latitude and the other at the corresponding south latitude. With this arrangement two marginal triangulations are possible as shown in Figure 6.3.2-1.

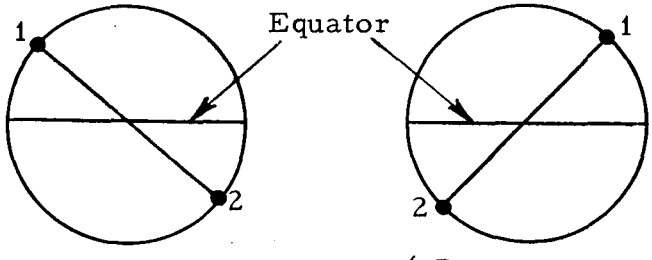

Figure 6.3.~~2-1~~ 1-3

The coverages of the two stations do not actually overlap, but it has been shown that an actual overlap is not necessary. The choice of one positive and one negative latitude gives triangulation in two roughly perpendicular planes when the vehicle is near the equatorial plane.

Two stations give only two triangulations every 24 hours. In order to achieve more triangulations, more stations must be used. If symmetry is to be preserved, the next step is to use four stations. These should be spaced

at 90-degree intervals in longitude and alternated in latitude. Then four triangulations per day are possible as shown in Figure 6.3.~~2-2~~ 1-4

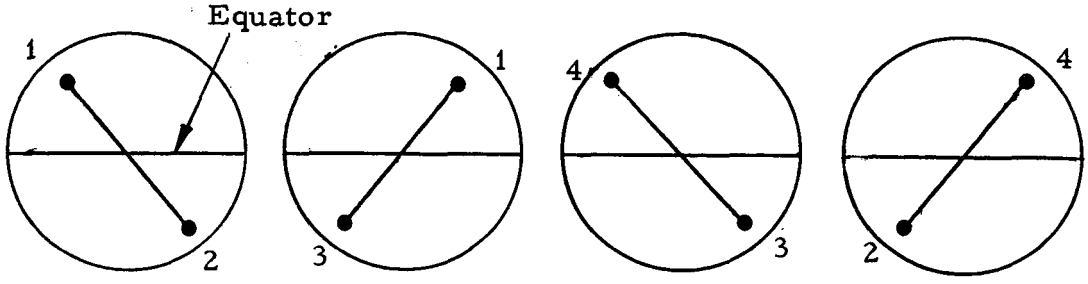

Figure 6.3.~~2-2~~ 1-4

If the latitudes of the stations are chosen properly, the triangulation planes can be made mutually perpendicular for a vehicle in the equatorial plane and far from the earth.

The use of four stations instead of two gives shorter baselines between the stations, but this should be more than offset by doubling the number of triangulation opportunities. In addition to the four triangulations already shown there are marginal triangulations involving three stations. One such possibility is shown in Figure 6.3.~~2-3~~ 1-5, where the earth has rotated 45 degrees from its first position in Figure 6.3.~~2-2~~ 1-4.

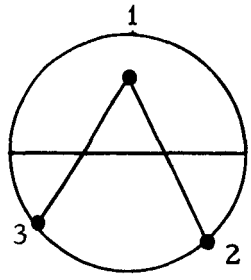

Figure 6.3.~~2-3~~ 1-5

Triangulations of this type are desirable since they allow position measurements in all three possible directions.

In this discussion it has been assumed for simplicity that tracking stations can be put anywhere on the earth. In actual practice, of course, this cannot be done. However, the principles associated with the ideal case above can be used to aid in the initial selection of locations for trial. The results of tracking accuracy analyses can then be used to select a good set from the constrained possibilities.

6.3.2 Usefulness of Optical Tracking Data

If both radar and optical tracking are used (with the accuracies assumed in this study) the optical tracking is most useful near the moon. Near the earth the radar accuracy is so good that optical data adds little information. Optical data in lunar orbit, for example, gives orientation information which is often better than radar can give. The optical observations also give information equally well for all orbit orientations, while the accuracy obtained from radar depends strongly on the orbit orientation.

The optical observations taken in the middle portions of both the translunar and transearth phases add little to the accuracy of prediction. This effect is discussed in more detail in the next section.

6.3.3 Distribution of Optical Data

The results of this study were obtained with optical data points uniformly distributed in time along the trajectory. It appears, however, that either fewer observations could be used or better accuracy could be obtained if optical observations were taken often when the vehicle is close to the landmarks and seldom when it is far from them. This conclusion can also be reached from examination of the variation of optical error with distance from the landmark and the curvature of the trajectory.

The error in the angle measured optically is assumed to be caused by a random instrument error and a landmark location uncertainty in the following way:

$$\sigma^2 = \sigma_I^2 + \left(\frac{\sigma_L}{r}\right)^2$$

or

$$\sigma = \sqrt{\sigma_I^2 + \left(\frac{\sigma_L}{r}\right)^2}$$

where

σ^2 = Variance of the observation

σ_I^2 = Variance of the instrument error

σ_L^2 = Variance of the landmark location

r = Distance from landmark to vehicle and $\frac{\sigma_L}{r} < 0.1$.

The magnitude of the partial derivative (in the direction of the gradient vector) of the observed angle with respect to the local position is $1/r$ (see Volume 1). Therefore the magnitude of the weighted partial is

$$\frac{1}{r\sqrt{\sigma_I^2 + \left(\frac{\sigma_L}{r}\right)^2}} \quad \text{or} \quad \frac{1}{\sqrt{r^2\sigma_I^2 + \sigma_L^2}}$$

If the landmark error dominates, that is

$(\sigma_L/r)^2 >> \sigma_I^2$, then the magnitude of the weighted partial is $1/\sigma_L$, independent of r. This is the case for small r. For large r, $\sigma_I^2 >> (\sigma_L/r)^2$, and the weighted partial is inversely proportional to r. Thus the accuracy of the optical observations is constant near the landmark and decreases as $1/r$ far from it. Therefore it is reasonable to take as much data as possible near the landmark and not so much far away. In addition to the better accuracy near the landmark, the trajectory normally has its greatest curvature there. This fact leads to independent gradient vectors for the observations and therefore reduces numerical difficulties.

REFERENCES

1. TRW/STL Report No. 8408-6040-RC-000, "Analysis of Apollo Orbit Determination Accuracy with Random Errors in Ground Based Radar and Onboard Optical Observations, Volume 1 - Introduction," dated April 10, 1964 (Conf.)

2. TRW/STL Report No. 8408-6041-RC-001, " ... Volume 2 - The Earth Parking Orbit," dated May 27, 1964 (Conf.)

3. TRW/STL Report No. 8408-6042-RC-000, " ... Volume 3 - The Trans-lunar Trajectory," dated May 4, 1964 (Conf.)

4. TRW/STL Report No. 8408-6043-RC-000, " ... Volume 4 - The Lunar Parking Orbit," dated February 24, 1964 (Conf.)

5. TRW/STL Report No. 8408-6044-RC-000, " ... Volume 5 - The Trans-earth Trajectory," dated May 15, 1964 (Conf.)

6. TRW/STL Report "Lunar Orbit Rendezvous Reference Trajectory Data Package (U) - Issue 2," dated September 30, 1963.

   Volume 1 - Report No. 8408-6023-RC-000, Summary and Reference Trajectory Data Exhibits (Conf.)

   Volume 2 - Report No. 8408-6024-RC-000, Printout Keys and Reference Trajectory Listing (Conf.)

   Volume 3 - Report No. 8408-6025-RC-000, Reference Trajectory Listing (Continued) (Conf.)

   Volume 4 - Report No. 8408-6026-RC-000, Reference Trajectory Listing (Concluded) (Conf.)